

Original Article

GSK3 β inhibition accelerates axon debris clearance and new axon remyelination

Yixun Chen^{1*}, Jian Weng^{1*}, Duanyang Han^{1,2*}, Bo Chen¹, Mingtai Ma¹, Youlai Yu¹, Ming Li¹, Zhongdi Liu¹, Peixun Zhang¹, Baoguo Jiang¹

¹Department of Orthopedics and Trauma, Peking University People's Hospital, Beijing, China; ²Department of Spine Surgery, Peking University Shenzhen Hospital, Shenzhen, China. *Equal contributors and co-first authors.

Received June 22, 2016; Accepted November 4, 2016; Epub December 15, 2016; Published December 30, 2016

Abstract: Glycogen synthase kinase 3 β (GSK3 β) inhibitors, especially the mood stabilizer lithium chloride, are also used as neuroprotective or anti-inflammatory agents. We studied the influence of LiCl on inducing early myelin clearance and on regulating the remyelination following peripheral nerves injury. We showed that the oral administration of adult mice with LiCl after sciatic nerve crush injury accelerated in vivo myelin debris clearance stimulated the expression of myelin proteins, restored the myelin structure, and accelerated the recovery of sciatic functions. LiCl treatment also promoted remyelination of the sciatic nerve after crush. Furthermore, we also demonstrated that LiCl exerts its action in Schwann cells by increasing the amount of β -catenin and provoking its nuclear localization in vivo. We showed by ChIP experiments that LiCl treatment drives β -catenin to bind to T-cell factor/lymphoid-enhancer factor response elements identified in myelin-related genes. Taken together, our results provide the first evidence that the GSK3 β could be considered as an important drug in inducing early myelin debris clearance and regulating the expression of myelin genes, which open new approaches in the clinical treatment of nerve injuries by utilizing GSK3 β inhibitors such as lithium.

Keywords: Peripheral nerve injury, GSK3 β , Wnt signals, LiCl, myelin clearance

Introduction

Peripheral nerve injuries are common in the realm of modern trauma medicine, but functional outcomes are often not satisfactory. Various conditions such as aberrant immune responses, local injury, ischemia, metabolic disorders, toxic agents, or viral infections may cause acquired neuropathies that significantly impair nerve regeneration capacity. To date, a few therapeutic treatments most of which are based on anti-inflammatory agents are available to promote delayed peripheral nerve repair.

Previous studies demonstrated that Schwann cells play an early role in removing myelin debris, which acts as an inhibitory agent to axons regeneration in the distal nerve. After axons disintegration, Schwann cell myelin sheath break apart longitudinally, forming small ovoid shaped myelin debris, which contains molecules that are inhibitory to axonal

growth including myelin-associated glycoprotein (MAG) and oligodendrocyte-myelin glycoprotein (OMgp) [1-3]. Of interest, Schwann cells play an active role in removing myelin debris derived from dying or damaged Schwann cells. In another word, Schwann cells can degrade their own myelin and phagocytose extracellular debris. Moreover, Schwann cells also express major histocompatibility complex (MHC) class II molecules; however, whether they can act as antigen presenting cells is not clear [4-6]. Perry and colleagues reported that denervated Schwann cells are the major phagocytic cells for the first 5 days after injury [7]. Although the role of Schwann cell in peripheral nerve repair is well addressed, regulation of Schwann cell behavior in peripheral nerve regeneration mechanism is still largely unknown.

LiCl is widely used as a long-term mood stabilizer in the treatment of bipolar and depressive disorders [8]. As an enzymatic inhibitor of GSK3 β , LiCl mimics the Wnt/ β -catenin signal-

GSK3 β inhibition accelerates debris clearance and remyelination

ing pathway. Growing evidence shows that LiCl has neuroprotective [9] and anti-apoptotic [10] properties, which can be used as a treatment in several neurodegenerative diseases such as Huntington disease [11], Alzheimer's disease [12], Parkinson disease [13] and in experimental autoimmune encephalomyelitis [14].

In this study, we report evidence that LiCl accelerates peripheral axon myelin debris clearance after peripheral nerve repair via activating Wnt/ β -catenin signaling in local Schwann cell. Most strikingly, LiCl oral administration promoted more rapid functional recovery of sciatic nerve crush injury. LiCl also provoked early elimination of local inhibitory molecule to axonal regrowth. Consequently, our findings open new perspectives in the treatment of acute peripheral nerve injury by administering GSK3 β inhibitors such as LiCl.

Material and methods

Ethics statement

The experimental procedures were carried out in accordance with the Chinese guidelines for the care and use of laboratory animals. The use of the animals was approved by the ethics committee and Experimental Animal Center of Peking University People's Hospital. All animal protocols were approved by the ethics committee of Peking University People's Hospital (Permit Number: 2011-16).

Mouse sciatic nerve injury

Mice were anesthetized, and sciatic nerves were exposed at approximately 1 cm distal to the sciatic notch. The nerve was crushed once for 60 seconds using microscopic needle holder. The crush site was marked by loosely placing a silk suture around the crush lesion and the wound was closed. Unlesioned negative controls were produced by exposing the nerve but leaving it uninjured.

Walking track analysis: sciatic functional index (SFI)

All animals underwent preoperative and postoperative walking track analysis in a fashion described previously for measuring SFI in the mouse. Briefly, the hind paws of each animal were moistened with water-soluble, non-toxic paint and the animals were allowed to walk

unassisted along a 6 \times 44 cm corridor lined with white paper. Prints for measurements were chosen at a point when the mouse was walking at a moderate pace. The tracks were evaluated for two different parameters: toe spread (TS), the distance between first and fifth toes and print length (PL), the distance between the third toe and the hind pad. Measurement of each parameter was made for the right (N: normal) and the left (E: experimental) paw prints. Using the parameters, preoperative and postoperative SFI for each animal was determined by the formula $118.9 \times \{(ETS-NTS)/NTS\} - 51.2 \times \{(EPL-NPL)/NPL\} - 7.5$ as described previously [15].

Foot base angle

Following sciatic nerve injury, impaired bending of the knee results in plantar flexion of the ankle joint during load bearing movements. With the classical beam-walk test, this response can be quantified by measuring the angle at which the sole of the hind paw meets the surface when the contralateral leg is lifted, termed the foot base angle [16]. During complete load bearing movements, the hind paw is externally rotated in the transverse plane in intact animals. However, one week following injury, the hind paw is externally rotated due to a loss in quadriceps innervation. Animals (n=10-12 per experimental condition) were trained to walk across a 1 m long ruler beam towards their home cage. Mice were filmed from the rear using a high-speed camera (A602fc, Basler) prior to the injury and at 1, 2, 3 weeks following injury. The locomotion videos were analyzed using single frame motion analysis (SFMA) using Simi Motion (SIMI Reality Motion Systems). The foot base angle was measured at a specific stage of the gait cycle where the contralateral leg was at its highest point, which is when the injured leg bears the most weight. The foot base angle was determined by dividing the left hind sole into two halves and measuring the angle of that line with the horizontal.

Western blot analysis

Western blots were performed as described [17]. Four mice in each group at 1-week post injury were harvested for examination of MPZ, PMP22, and Oct6 and Sox10 proteins. These specimens were homogenized with tissue protein extraction reagent T-PERTM (Pierce, USA) containing phosphatase and protease inhibi-

GSK3 β inhibition accelerates debris clearance and remyelination

tors. The protein samples (30 μ g) were resolved on 10% SDS-polyacrylamide gels and transferred to polyvinylidene difluoride membranes. Blots were blocked with 5% skim milk in Tween-20/phosphate-buffered saline, and incubated with various primary antibodies as: rabbit anti-Sox10 (ab27655 from Abcam, USA), anti-Oct6 (ab31766, from Abcam, USA), anti-MPZ (ab31851, from Abcam, USA), anti-PMP22 (sc-515199, from Santa, USA) and mouse anti- β -actin (Millipore Biotechnology, USA) at 4°C overnight. The blots were then incubated with HRP-conjugated secondary antibodies at room temperature for 60 minutes, and developed with ECLTM Western Blotting Systems (Amersham Pharmacia Biotech, UK). The protein bands were quantified with FluorChem 8900 imaging system and the AlphaEaseFC software (Alpha Innotech Corp, USA).

Osmic acid staining

Nerve tissue was harvested at WPI1, WPI2 and WPI3 time points respectively. Tissues were then fixed in 4% paraformaldehyde in 0.1 M phosphate buffer for 24 h at 4°C. The nerves were then rinsed twice in water for 12 h. Nerve segments were cut 5 mm distal to the lesion site. Each sample was stained in 1% osmium tetroxide for 12 h, then dehydrated through a graded series of ethanols and the specimens were then immersed in xylene, embedded in paraffin, then each nerve segment was sliced into 5 μ m cross-sections with a Leica tissue microtome. Images from were acquired under a microscope, from which the total number of myelinated axons in each segment was counted by Image J software. Morphometric measurements were also performed by Image J software. The shortest lengths of the inner and outer margins of the myelin sheath were measured to determine the axon diameter and fiber diameter. After obtaining the axon and fiber diameter, myelin thickness and G-ratio were calculated. Subsequently, a set of five non-overlapping fields was used to evaluate fiber diameter distribution by a random pick from each section. The evaluated area covered approximately 60% of the total area per section.

Immunohistochemistry staining

β -catenin and NF κ B-p65 were detected on formalin-fixed, paraffin-embedded sections by us-

ing primary antibodies (anti- β -catenin, 610153, from BD, USA) (anti-NF κ B-p65, ab16502, from Abcam, USA), slides were baked at 55°C for overnight, deparaffinized in two washes of xylene, and rehydrated in a decreasing ethanol gradient. Antigen retrieval was performed using 0.5% trypsin for 30 min at 37°C in a humidified chamber. Endogenous peroxidases were deactivated with 3% H₂O₂ for 30 min, and sections were blocked in PBS supplemented with 0.1% Triton-X (Sigma, USA), 2% goat serum (Gibco, USA), and 1% BSA (Sigma, USA) for 20 min at room temperature. Sections were incubated with primary antibody (1:300 dilution for anti- β -catenin; 1:2000 dilution for anti-NF κ B-p65) in Antibody dilution water overnight at 4°C. The following morning, the sections were washed in PBS and incubated with anti-mouse IgG-HRP secondary antibody (GTVision, China) in PBS (1:1000 dilution) for 45 min at room temperature. After washing with PBS, HRP activity was detected using a DAB substrate kit (SK-4100; Vector Laboratories) according to the manufacturer's instructions.

Chromatin immunoprecipitation

Next, we performed chromatin immunoprecipitation (ChIP) assays in S16 Schwann cell line (ATCC, USA). Briefly described as follow. Conventional formaldehyde cross-linking was performed by incubating the cells in freshly prepared buffered formaldehyde (50 mM Hepes KOH pH 7.5, 100 mM NaCl, 1 mM EDTA, and 0.5 mM EGTA, 1% formaldehyde) for 10 minutes. Schwann cells from control and LiCl-treated groups were scraped respectively in cold PBS and spun at 2000 rpm for 5 minutes. The cell pellet was resuspended in SDS lysis buffer (1% SDS, 10 mM EDTA, 50 mM Tris pH 8.0) and subsequently sonicated for 15 cycles with 15-s on and 30-s off regime. Sheared chromatin was pre-cleared with protein A Agarose/Salmon sperm DNA (Millipore Biotechnology, USA) for one hour. 1% chromatin was set aside to serve as a 1/100th of total chromatin input control. After centrifugation, the supernatant was incubated with 10 μ g of anti-Sox10, anti-MPZ, anti-PMP22 antibody (Abcam, USA) or 10 μ g of normal mouse immunoglobulin G (IgG; Santa Cruz Biotechnology, USA) control antibody at 4°C on a rotating wheel overnight. Subsequently, immune complexes were incubated with 60 μ l of protein A Agarose/

GSK3 β inhibition accelerates debris clearance and remyelination

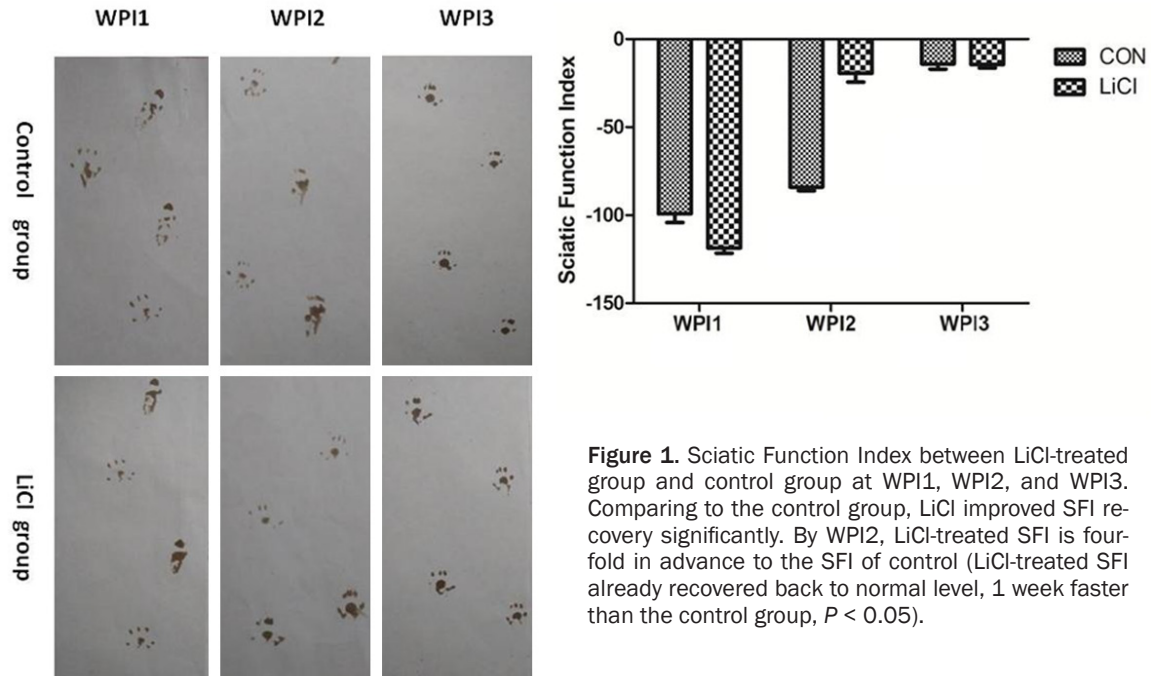


Figure 1. Sciatic Function Index between LiCl-treated group and control group at WPI1, WPI2, and WPI3. Comparing to the control group, LiCl improved SFI recovery significantly. By WPI2, LiCl-treated SFI is four-fold in advance to the SFI of control (LiCl-treated SFI already recovered back to normal level, 1 week faster than the control group, $P < 0.05$).

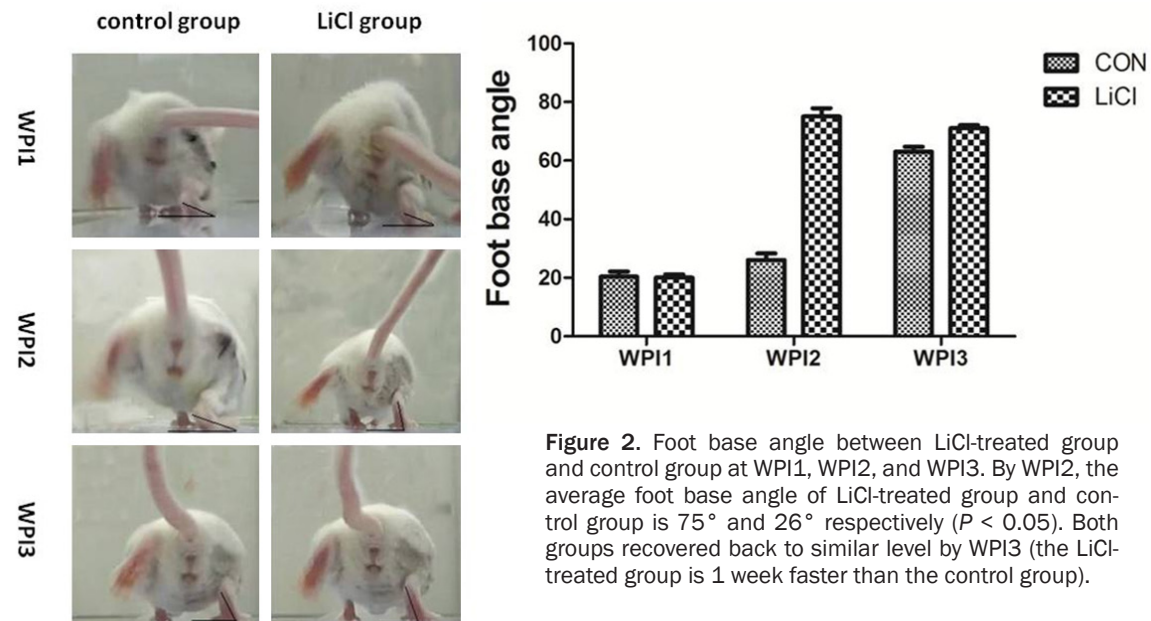


Figure 2. Foot base angle between LiCl-treated group and control group at WPI1, WPI2, and WPI3. By WPI2, the average foot base angle of LiCl-treated group and control group is 75° and 26° respectively ($P < 0.05$). Both groups recovered back to similar level by WPI3 (the LiCl-treated group is 1 week faster than the control group).

Salmon sperm DNA slurry for one hour. Next, immunoprecipitated chromatin was eluted twice each time with 250 μ l of elution buffer (1% SDS, 0.1 M NaHCO₃). The elutions were pooled and 5 M NaCl was added to a final concentration of 300 mM. Further, cross-links were reversed by incubating the sample at 65°C for 5 hours. The solution was adjusted to 10 mM EDTA and 10 mM Tris-HCl pH 6.5. ProteinaseK (10 mg/ml) was added to 40 μ g/

ml and the solution was incubated for one hour at 45°C. DNA was purified with phenol: chloroform: isoamyl alcohol, precipitated with EtOH and dissolved in water. The same reverse cross-linking and purification procedure was followed for the input sample. Comparative Ct values were used to calculate the enrichment of a DNA segment relative to the total input. RT-PCR analysis of inputs or immunoprecipitated DNAs was performed.

GSK3 β inhibition accelerates debris clearance and remyelination

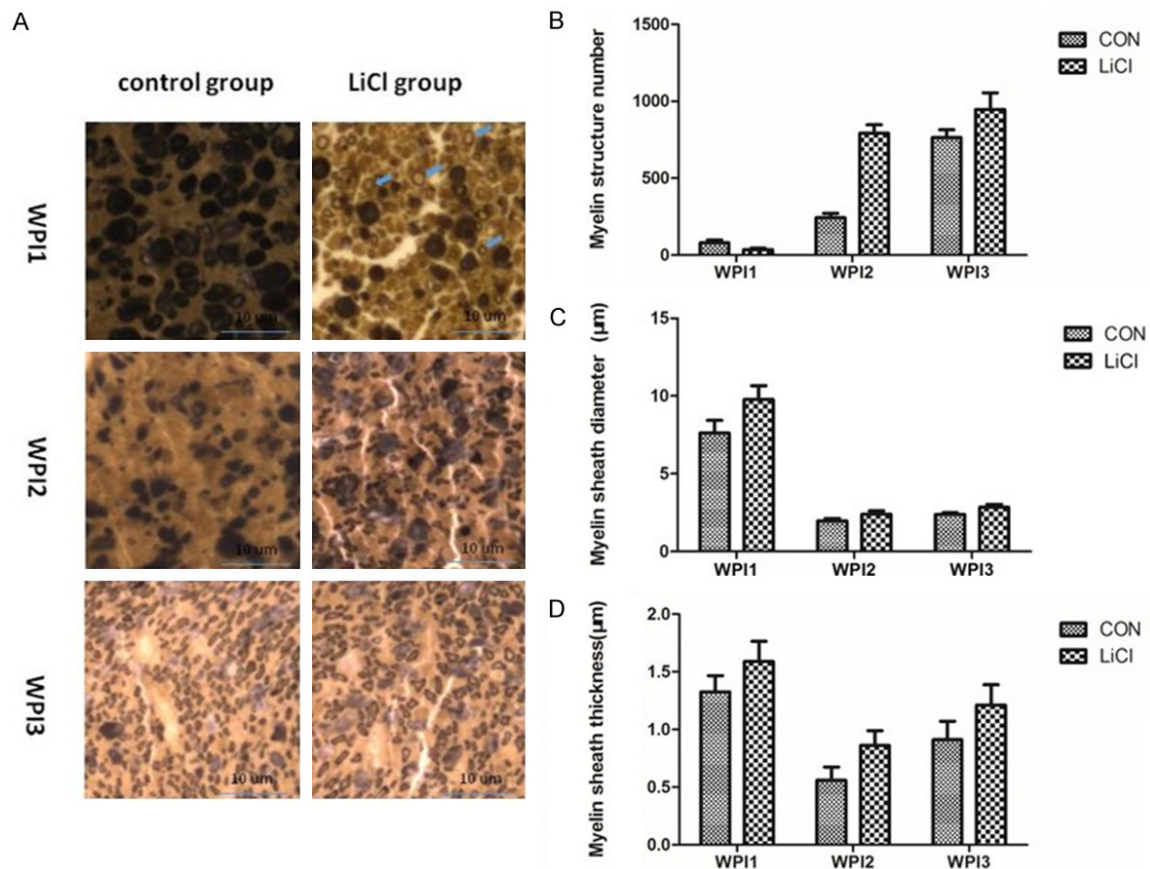


Figure 3. A. Osmic acid staining between LiCl-treated group and control group at WPI1, WPI2, and WPI3. Comparing to control group at WPI1, LiCl-treated group has already started to clear myelin debris, meanwhile begun to regrow new myelin sheath (shown by arrows). By WPI2 the myelin clearance of control group has done and thin myelin sheath axon started to sprout (1 week slower than LiCl-treated group), while the regeneration process was about to finish in the LiCl-treated group. Both groups showed well-regenerated axon structure with similar parameters at WPI3. B. Myelin sheath structure number between LiCl-treated group and control group at WPI1, WPI2, and WPI3. A significant difference of myelin sheath structure number was shown between two groups at each time point ($P < 0.05$). LiCl promoted newly sprouted axon (indicated by larger myelinated structures number) to regrow into the distal nerve stumps. C. Myelin sheath diameter between LiCl-treated group and control group at WPI1, WPI2, and WPI3. By WPI1 to WPI3, the average diameter of myelin sheath in LiCl group was significantly bigger ($P < 0.05$), LiCl accelerated the regrow of new axon. D. Myelin sheath thickness between LiCl-treated group and control group at WPI1, WPI2, and WPI3. Comparing to the control group at each time point, the average myelin thickness of LiCl-treated group is significantly thicker ($P < 0.05$), LiCl enhanced *in vivo* nerve remyelination.

Statistical analysis

Statistical analyses were performed using SPSS 20.0 (SPSS Inc., Chicago, IL, USA). All the results were presented as mean \pm standard error. An overall analysis of the differences between group means was calculated by t-test. A probability of $P < 0.05$ was considered significant for all statistical comparisons.

Results

LiCl oral administration accelerates sciatic nerve crush injury functional recovery

To assess the outcome of the oral administration of LiCl, a well-established inhibitor of GSK3 β ,

after peripheral nerve crush injury, we performed sciatic nerve crush in mice model that provokes a local demyelination and subsequent palsy of the ipsilateral (crushed) hind limb. The right sciatic nerve was crushed whereas the left one was left intact to serve as a control. We then analyzed sciatic function index (SFI) and foot base angle between LiCl-treated and control groups at different post-lesion time points [1, 2 and 3 week post injury (WPI1, WPI2, and WPI3)]. In the LiCl-treated group, animals were treated with LiCl (0.2%) in drinking water (each mouse intake 4-7 ml per day) immediate following nerve crush and kept during the time until euthanasia. In the control group, 0.2% NaCl was used to replace LiCl during a similar period.

GSK3 β inhibition accelerates debris clearance and remyelination

Table 1. Morphometric measurements in different groups 3 weeks post-injury

	Control group	LiCl group
Number of slices per segment	5	5
Number of axons per slice	100	100
Fiber diameter (μm)	2.42 \pm 0.31	2.86 \pm 0.24*
Axon diameter (μm)	1.33 \pm 0.11	1.76 \pm 0.27*
G-ratio (Axon diameter/Fiber diameter)	0.55 \pm 0.03	0.61 \pm 0.04*
Myelin thickness (μm)	0.91 \pm 0.18	1.21 \pm 0.25*
Myelinated axons percentage	63.83 \pm 6.80	77.08 \pm 10.02*

* $P < 0.05$ versus control group.

As shown in **Figure 1**, walking track test showed that LiCl-treated mice exhibited markedly improved SFI recovery comparing to control counterparts. By WPI2, LiCl-treated SFI is four-fold in advance to the SFI of control mice. (**Figure 1**, $P < 0.05$) LiCl-treated SFI already recovered back to normal level, whereas the control group is 1 week slower in SFI restoration. By WPI3, we can consider that the animal recovered completely since we did not observe any significant SFI difference between the control animals and LiCl-treated ones. Similarly, foot base angle analysis demonstrated that, by WPI2, the average foot base angle of LiCl-treated animal recovered back to 75°, comparing to 26° of control group (**Figure 2**, $P < 0.05$) By WPI3, the control mice foot angle increased to 63°, indicating a similar 1 week lag in foot angle healing. In conclusion, our results indicate that LiCl markedly accelerates the functional recovery of sciatic nerve function after crush injury in mice.

LiCl accelerates early myelin debris clearance

To evaluate in vivo myelin debris clearance, we performed osmic acid staining. Our data showed that LiCl oral treatment promoted axonal myelin debris early removal. At WPI1, the majority of the myelin sheath structure still could be observed from control group indicating that the myelin debris clearance process was barely begun. (**Figure 3A** upper-left) On the contrary, in LiCl treatment group at WPI1, it could be observed that majority of the myelin sheath structures had already been removed leaving only a few tiny myelinated structures. (**Figure 3A** upper-right with arrow heads) To confirm our observation, we perform axon counting test to quantify our findings. As shown

in **Figure 3B**, the average residue myelin sheath structure number was significantly reduced after one week of treatment with oral LiCl: 36 with NaCl vs. 79 with LiCl (per 40x field). It could be observed that, by WPI2, myelin debris clearance had been largely well finished in LiCl group, whereas myelin debris clearance process was merely initiated in NaCl control group. Furthermore, by WPI1, the average diameter of the myelin sheath in LiCl group was significantly bigger (7.6 μm with

NaCl vs. 9.8 μm with LiCl) (**Figure 3C**) and the average myelin thickness is significantly thicker: 1.32 μm with NaCl vs. 1.59 μm with LiCl. (**Figure 3D**) These findings suggested that newly sprouted axon (indicated by tiny myelinated structures with thin myelin sheath) had started to regrow into the distal nerve stumps in LiCl group. At WPI1, the crushed nerves of LiCl-treated mice exhibited a thinner myelin sheath with a smaller diameter (**Figure 3A** upper right), suggesting accelerated myelin debris removal promote early axon regeneration. By the end of WPI2, the laggard myelin clearance in the control group was done and small diameter with thin myelin sheath axon started to sprout into the distal nerve stump. (**Figure 3A** middle left) However, by the same WPI2 time point, the regeneration process was about to finish in LiCl group and the morphology of the injured nerve was mostly recovered back to normal. (**Figure 3A** middle right). At WPI3, both LiCl and control group showed well-regenerated axon structure with similar parameters. (**Figure 3A** lower right & left) In conclusion, as evidenced by our data, LiCl oral administration accelerates the myelin debris clearance after sciatic nerve crush injury and improves the nerve repair process. Early finished myelin debris clearance advanced the nerve phenotype recovery.

LiCl promotes both in vivo and vitro remyelination

Next, we analyzed the structure of sciatic nerve at WPI3 by staining myelin substance using osmic acid staining. The crushed sciatic nerves of LiCl-treated mice exhibited a thicker myelin sheath (**Figure 3D**), suggesting enhanced in vivo nerve remyelination. In accordance, g-ratio

GSK3β inhibition accelerates debris clearance and remyelination

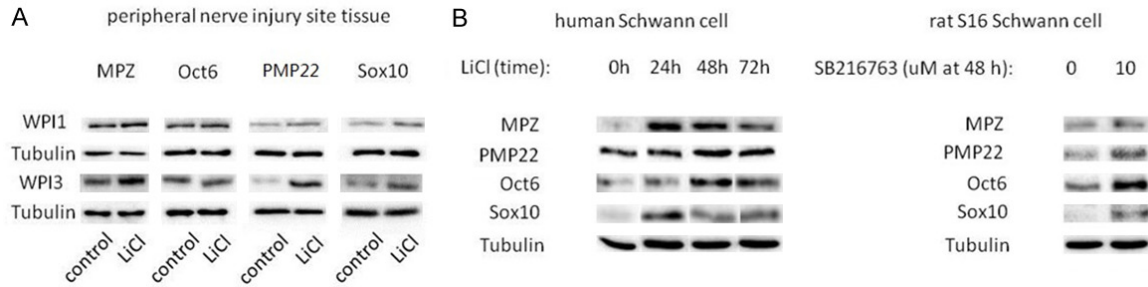


Figure 4. A. Western blot analyses of MPZ, Oct6, PMP22 and Sox10 from injury nerve tissue between LiCl-treated group and control group at WPI1 and WPI3. Comparing to control animal MPZ, PMP22 and Sox10 protein expression from the LiCl-treated group was upregulated at both WPI1 and WPI3 time points, demonstrated that LiCl contributes to boosting early and upregulated myelin protein formation in vivo. B. Western blot analyses of MPZ, PMP22, Oct6 and Sox10 from human and rat Schwann cell after GSK3β inhibition by LiCl and SB216763 treatment respectively. By LiCl presence, MPZ and Sox10 protein expression reach an apex at 24 hours after treatment. PMP22 and Oct6 expression level reached an apex at 48 hours. Similarly, by SB216763 treatment, all four marker protein levels were significantly elevated by 10 uM of SB216763 presence in S16 Schwann cell line.

calculation (defined as axon diameter/myelin sheath diameter) further reinforced this notion. Specifically, the g-ratio of LiCl-treated animals was significantly higher than that of control animals (0.61 ± 0.04 with LiCl vs 0.55 ± 0.03 with NaCl, $P < 0.05$, **Table 1**). Furthermore, myelinated axons percentage was higher in the LiCl-treated group (77.08 ± 10.02 with LiCl vs 63.83 ± 6.80 with NaCl, $P < 0.05$, **Table 1**). In addition, we analyzed the expression of myelin proteins (MPZ and PMP22) and remyelination transcription factors (Oct6 and Sox10) by western blot (**Figure 4A**). As our data showed, comparing to control animal, the MPZ level of injured sciatic nerve from LiCl treatment group had an increase at WPI1. Likewise, Oct6, PMP22 and Sox10 level in LiCl group were slightly upregulated by WPI1. By WPI3, MPZ, PMP22 and Sox10 expression level in LiCl-treated mice was significantly increased as compared to control mice, indicating more robust local remyelination in LiCl-treated animals over control ones. Furthermore, we tested LiCl treatment on in vitro cultured Schwann cell lines. As shown in **Figure 4B**, our data showed a 50 mg/kg/d i.p. injection of LiCl in vitro treatment elevated human Schwann cell MPZ expression by 24 hours of treatment. Then, MPZ expression began to decline with accumulative treating time. Similarly, Sox10 protein expression also reaches an apex at 24 hours after treatment. Nonetheless, PMP22 and Oct6 expression level reached an apex at 48 hours after treatment. Moreover, we also tested alternative GSK3β inhibitor SB216763 (Sigma,

USA). Our data confirmed that SB216763 exhibited a similar effect on Rat S16 Schwann cell line. By 48 hours treatment, all four marker protein levels were significantly elevated by 10 uM of SB216763 presence. Collectively, our data demonstrated LiCl oral administration contributes to an early and strong upregulated myelin structure protein formation in vivo. Taken together, our data demonstrated that LiCl treatment promotes in vivo remyelination and myelin protein production.

LiCl promotes β-catenin nuclear localization

Next, we performed immunohistochemistry staining to detect β-catenin and NFκB-p65 expression in injured nerve during the repair process. As shown in **Figure 5A**, by WPI1, the overall β-catenin expression in local nerve tissue is largely upregulated in LiCl treatment group. Furthermore, comparing to control group, we observed elevated β-catenin nuclear concentration in LiCl treatment group. Similar high level β-catenin nuclear localization persists through WPI2 and drop back to normal range by WPI3. Our result showed that LiCl oral administration enhances in vivo β-catenin expression and nuclear localization in the early post-injury period. Also, we performed NFκB-p65 staining. We found that LiCl treatment does not have an obvious impact on NFκB-p65 overall expression and nuclear concentration (**Figure 5B**). The NFκB-p65 expression was slightly elevated by WPI1 and faded from WPI2. There are no significant differences between LiCl and control group at all three-time

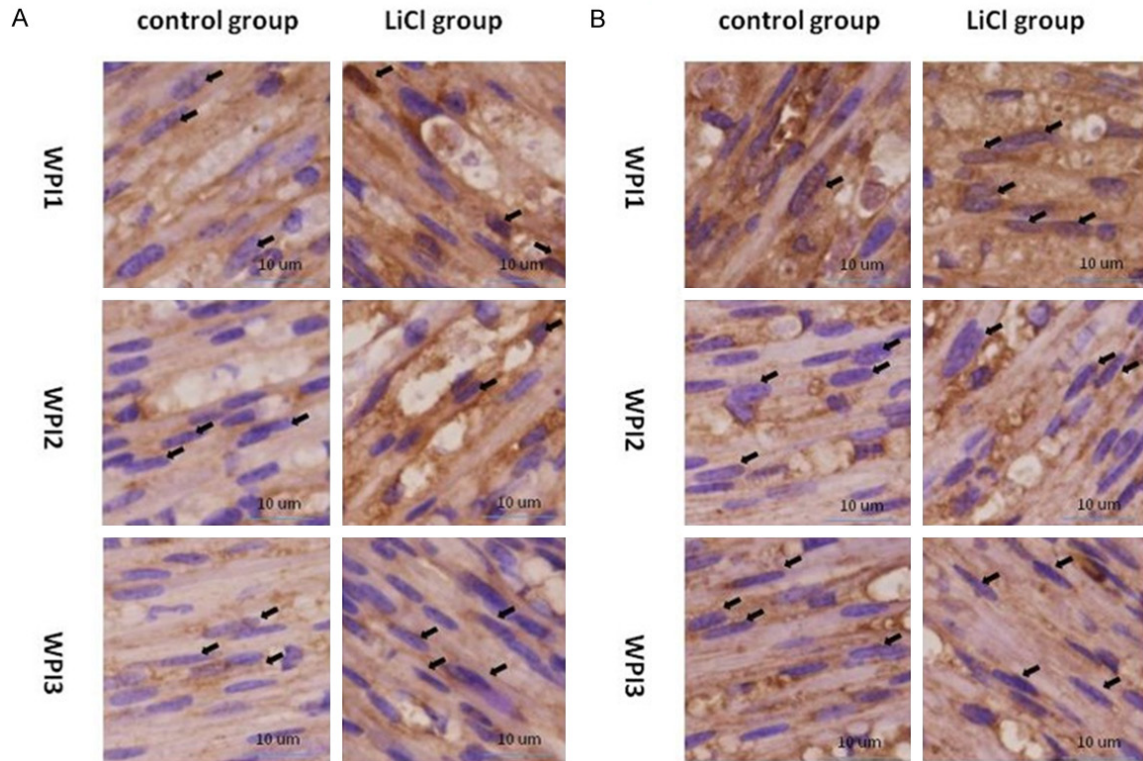


Figure 5. A. Immunohistochemistry staining of β -catenin between LiCl-treated group and control group at WPI1, WPI2, and WPI3. Comparing with the control group, significant elevated overall β -catenin expression and nuclear localization (shown by arrows) was observed in LiCl group at WPI1 and WPI2 respectively. From WPI3 time point, both overall expression and nuclear localization began to decrease. B. Immunohistochemistry staining of NF κ B-p65 between LiCl-treated group and control group at WPI1, WPI2, and WPI3. No significant difference was shown between LiCl and control group at all three-time points concerning NF κ B-p65 overall expression and nuclear concentration (shown by arrows).

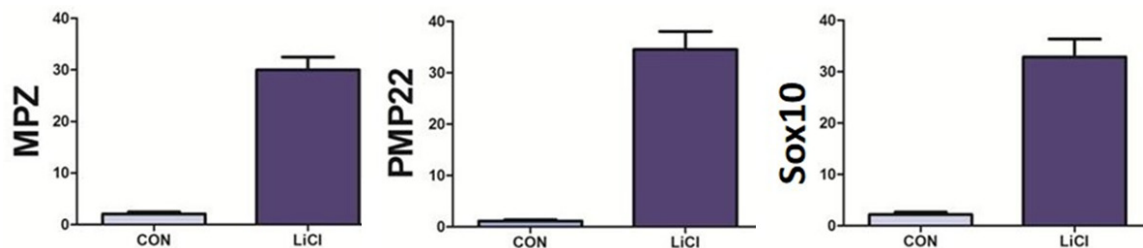


Figure 6. ChIP analyses of MPZ, PMP22, and Sox10 between LiCl-treated group and control group. LiCl promotes β -catenin recruitment on TCF/LEF binding site of myelin genes (MPZ was enhanced by 15 folds, PMP22 by 30 folds and Sox10 by 15 folds respectively after 1 h, $P < 0.05$).

points. Thus, our results demonstrated that LiCl administration most possibly exerted its efficacy via Wnt activation mechanism other than NF κ B signaling.

Subsequently, we performed ChIP assay to identify the molecular targets of LiCl at the level of MPZ, PMP22, and Sox10 promoters. Previous studies have already shown that MPZ,

PMP22, and Sox10 promoters contain active TCF/LEF-binding sites (**Figure 6**). ChIP analysis demonstrated that β -catenin recruitment by TCF/LEF binding domain (localized -8,487/-8,471 bp on the level of the MPZ promoter) was enhanced by 15 folds after 1 h of LiCl treatment. Also, we identified a potential binding site of TCF/LEF in position +107/+124 on PMP22 promoter region. Our result showed

GSK3 β inhibition accelerates debris clearance and remyelination

that β -catenin recruitment increased by 30 folds after 1 h of incubation with LiCl. As for Sox10 promoter, our data illustrated that β -catenin recruitment increased by 15 folds after 1 h of incubation with LiCl. Collectively, our data proved that LiCl delivers myelination enhancement effect through promoting β -catenin recruitment on TCF/LEF binding site of myelin genes.

Discussion

In recent decades, GSK3 β emerged as a promising drug target in treating cancer [18] and central nerve disorders [19]. Lithium chloride is a well-established GSK3 β inhibitor which has been widely utilized in treating bipolar disease [20, 21]. Recently, multiple *in vitro* and *in vivo* studies reported that lithium chloride exhibit prominent effect in treating acute brain injuries (such as cerebral ischemia) and neurodegenerative disorders (such as Huntington disease, Parkinson disease, and Alzheimer's disease) [14, 22]. Clinically, lithium chloride draws neuro-protective effect by inhibiting neuron apoptosis and promoting neurogenesis simultaneously [10]. For instance, lithium protected neurons from apoptosis *in vitro* neuron cell cultures against over-does glutamate presence. Moreover, lithium was also shown to reduce NMDA receptor agonist-induced striatal lesion in a Huntington disease model [11] via inhibiting GSK3 β . Furthermore, besides reducing brain damage, Lithium is also known to promote neuron survival, proliferation, and neural progenitor differentiation [23]. Also, Lithium chloride increases cell survival gene expression, namely β -catenin, Hsp70, BDNF, and Bcl-2 [24-26]. Additionally, lithium also exhibits an anti-inflammatory effect in the cerebral tissue [27]. However, the effect of wide spectrum GSK3 β inhibitors on remyelination and myelin clearance of the peripheral nervous system is still unexplored.

Therefore, we performed nerve crush on the sciatic nerve to study the effect of LiCl on remyelination after myelin injuries. We have tested two different peripheral nerves to demonstrate that the beneficial effects of lithium on remyelination are not limited a specific type of nerve. We gave oral administered LiCl to verify its effects on myelin debris clearance and remyelination. Indeed, at this stage of regeneration, the remyelination of the regrowing axons has

started and in addition, myelin debris has been removed by macrophages and Schwann cells, allowing to precisely evaluate the formation of new myelin. In this experiment, we also tested the efficacy of orally administered LiCl (added to drinking water) because patients receive lithium orally.

In our crush nerve injury model, LiCl administration accelerated the recovery of SFI and foot base angle parameter in injured animals. Moreover, LiCl markedly improved myelin debris clearance after nerve injury. The LiCl group out raced the control by a week. By two week after the crush, lithium-treated animals had practically totally recovered, whereas NaCl-treated ones still had a palsy of the hind limb. LiCl greatly ameliorated the phenotype of the lesioned nerve: it enhanced the expression of myelin proteins and increased the thickness of the myelin sheaths, as indicated by the decrease of the g-ratio. Consequently, after LiCl administration, the number of myelinated axons was doubled. These encouraging results demonstrate that the oral administration of lithium has beneficial effects in the treatment of myelin injuries.

To illustrate the mechanism by which LiCl exert its efficacy, we performed immunohistochemistry staining and our results showed that LiCl treatment largely increases β -catenin overall expression and nuclear localization which is the landmark molecular event of Wnt signaling pathway. Moreover, our data showed that LiCl treatment does not likely to exert its efficacy through NF κ B mechanism since p65 expression and nuclear concentration level was not differentiated between LiCl and control group. This finding suggested that LiCl's axon debris clearance promotion function is not due to NF κ B and inflammation activation.

Subsequently, we ask: Does LiCl exerts its positive effects on Schwann cells? The treatment of cells significantly enhanced the expression and nuclear localization of β -catenin and stimulated a TCF/LEF-containing promoter. Therefore, the stimulation of MPZ, PMP22 and Sox10 is not a result of the activation of the Akt pathway but rather of β -catenin/TCF signaling. The nuclear stabilized β -catenin binds to TCF/LEF transcription factors present in the vicinity of Sox10, PMP22, and MPZ promoters, as suggested by ChIP assays. Those observations are

GSK3 β inhibition accelerates debris clearance and remyelination

in accordance with our previous results showing that the Wnt/ β -catenin pathway is essential for myelin gene expression.

In conclusion, we first demonstrated that GSK3 β inhibitors accelerate myelin debris clearance and enhance remyelination process after peripheral nerve injury. Our results provide the first evidence that the GSK3 β could be considered as an important pharmaceutical target in inducing early myelin debris clearance and regulating the expression of myelin genes. Our discoveries open new approaches in the clinical treatment of nerve injuries by utilizing GSK3 β inhibitors such as lithium.

Acknowledgements

This work was funded by Chinese National Ministry of Science and Technology 973 Project Planning (No. 2014CB542200); 863 project (SS2015AA020501), the ministry of education innovation team (IRT1201); the National Natural Science Fund (No. 31571235, 31571236, 31271284, 31171150, 81171146, 30971526, 31100860, 31040043), the Educational Ministry New Century Excellent Talents Support Project (No. BMU20110270) and The ministry of health of the public welfare industry special scientific research (201302007).

Disclosure of conflict of interest

None.

Address correspondence to: Peixun Zhang and Baoguo Jiang, Department of Orthopedics and Trauma, Peking University People's Hospital, Beijing, China. E-mail: zhangpeixun@bjmu.edu.cn (PXZ); jiangbaoguo@vip.sina.com (BJG)

References

- [1] Stoll G, Griffin JW, Li CY and Trapp BD. Wallerian degeneration in the peripheral nervous system: participation of both Schwann cells and macrophages in myelin degradation. *J Neurocytol* 1989; 18: 671-683.
- [2] Huang JK, Phillips GR, Roth AD, Pedraza L, Shan W, Belkaid W, Mi S, Fex-Svenningsen A, Florens L, Yates JR 3rd and Colman DR. Glial membranes at the node of Ranvier prevent neurite outgrowth. *Science* 2005; 310: 1813-1817.
- [3] Shen ZL, Lassner F, Bader A, Becker M, Walter GF and Berger A. Cellular activity of resident macrophages during Wallerian degeneration. *Microsurgery* 2000; 20: 255-261.
- [4] Meyer Zu Hörste G, Hu W, Hartung HP, Lehmann HC, Kieseier BC. The immunocompetence of Schwann cells. *Muscle Nerve* 2008; 37: 3-13.
- [5] Hirata K, Mitoma H, Ueno N, He JW and Kawabuchi M. Differential response of macrophage subpopulations to myelin degradation in the injured rat sciatic nerve. *J Neurocytol* 1999; 28: 685-695.
- [6] Holtzman E and Novikoff AB. Lysosomes in the rat sciatic nerve following crush. *J Cell Biol* 1965; 27: 651-669.
- [7] Perry VH, Tsao JW, Fearn S and Brown MC. Radiation-induced reductions in macrophage recruitment have only slight effects on myelin degeneration in sectioned peripheral nerves of mice. *Eur J Neurosci* 1995; 7: 271-280.
- [8] Phiel CJ and Klein PS. Molecular targets of lithium action. *Annu Rev Pharmacol Toxicol* 2001; 41: 789-813.
- [9] Zhong J, Yang X, Yao W and Lee W. Lithium protects ethanol-induced neuronal apoptosis. *Biochem Biophys Res Commun* 2006; 350: 905-910.
- [10] Chuang DM. The antiapoptotic actions of mood stabilizers: molecular mechanisms and therapeutic potentials. *Ann N Y Acad Sci* 2005; 1053: 195-204.
- [11] Wei H, Qin ZH, Senatorov VV, Wei W, Wang Y, Qian Y and Chuang DM. Lithium suppresses excitotoxicity-induced striatal lesions in a rat model of Huntington's disease. *Neuroscience* 2001; 106: 603-612.
- [12] Noble W, Planel E, Zehr C, Olm V, Meyerson J, Suleman F, Gaynor K, Wang L, LaFrancois J, Feinstein B, Burns M, Krishnamurthy P, Wen Y, Bhat R, Lewis J, Dickson D and Duff K. Inhibition of glycogen synthase kinase-3 by lithium correlates with reduced tauopathy and degeneration in vivo. *Proc Natl Acad Sci U S A* 2005; 102: 6990-6995.
- [13] Youdim MB and Arraf Z. Prevention of MPTP (N-methyl-4-phenyl-1, 2, 3, 6-tetrahydropyridine) dopaminergic neurotoxicity in mice by chronic lithium: involvements of Bcl-2 and Bax. *Neuropharmacology* 2004; 46: 1130-1140.
- [14] De Sarno P, Axtell RC, Raman C, Roth KA, Alessi DR and Jope RS. Lithium prevents and ameliorates experimental autoimmune encephalomyelitis. *J Immunol* 2008; 181: 338-345.
- [15] Inserra MM, Bloch DA and Terris DJ. Functional indices for sciatic, peroneal, and posterior tibial nerve lesions in the mouse. *Microsurgery* 1998; 18: 119-124.
- [16] Irintchev A, Simova O, Eberhardt KA, Morellini F and Schachner M. Impacts of lesion severity

GSK3 β inhibition accelerates debris clearance and remyelination

- and tyrosine kinase receptor B deficiency on functional outcome of femoral nerve injury assessed by a novel single-frame motion analysis in mice. *Eur J Neurosci* 2005; 22: 802-808.
- [17] Tawk M, Makoukji J, Belle M, Fonte C, Trousson A, Hawkins T, Li H, Ghandour S, Schumacher M and Massaad C. Wnt/beta-catenin signaling is an essential and direct driver of myelin gene expression and myelinogenesis. *J Neurosci* 2011; 31: 3729-3742.
- [18] Takahashi-Yanaga F and Sasaguri T. Drug development targeting the glycogen synthase kinase-3beta (GSK-3beta)-mediated signal transduction pathway: inhibitors of the Wnt/beta-catenin signaling pathway as novel anticancer drugs. *J Pharmacol Sci* 2009; 109: 179-183.
- [19] Bhat RV, Budd HS and Avila J. Glycogen synthase kinase 3: a drug target for CNS therapies. *J Neurochem* 2004; 89: 1313-1317.
- [20] Gould TD, Chen G and Manji HK. In vivo evidence in the brain for lithium inhibition of glycogen synthase kinase-3. *Neuropsychopharmacology* 2004; 29: 32-38.
- [21] Pies R. Combining lithium and anticonvulsants in bipolar disorder: a review. *Ann Clin Psychiatry* 2002; 14: 223-232.
- [22] Zhong J and Lee WH. Lithium: a novel treatment for Alzheimer's disease. *Expert Opin Drug Saf* 2007; 6: 375-383.
- [23] Su H, Chu TH and Wu W. Lithium enhances proliferation and neuronal differentiation of neural progenitor cells in vitro and after transplantation into the adult rat spinal cord. *Exp Neurol* 2007; 206: 296-307.
- [24] Chuang DM. Neuroprotective and neurotrophic actions of the mood stabilizer lithium: can it be used to treat neurodegenerative diseases. *Crit Rev Neurobiol* 2004; 16: 83-90.
- [25] Adams JM and Cory S. The Bcl-2 protein family: arbiters of cell survival. *Science* 1998; 281: 1322-1326.
- [26] Sadoul R. Bcl-2 family members in the development and degenerative pathologies of the nervous system. *Cell Death Differ* 1998; 5: 805-815.
- [27] Basselin M, Villacreses NE, Lee HJ, Bell JM and Rapoport SI. Chronic lithium administration attenuates up-regulated brain arachidonic acid metabolism in a rat model of neuroinflammation. *J Neurochem* 2007; 102: 761-772.